Available online at www.sciencedirect.com
SCIENCE DIRECT®
ELSEVIER
Ocean Engineering 32 (2005) 1015–1036
OCEAN ENGINEERING
www.elsevier.com/locate/oceaneng

Distributions of extreme wave, crest and trough heights measured in the North Sea

Paul Stansell*

School of Physics, The University of Edinburgh, James Clerk Maxwell Building, The King's Buildings, Mayfield Road, Edinburgh EH9 3JZ, UK

Received 1 June 2004; accepted 6 October 2004
Available online 22 December 2004

Abstract

We present statistical analyses of the most extreme wave, crest and trough heights occurring during 793 h of surface elevation measurements collected during 14 severe storms in the North Sea. This data contains 104 freak waves. It is shown that the statistics of the extremes of crest and trough heights depends strongly on the significant wave height. Fitted statistical models are provided and a procedure presented whereby one may calculate good estimates of the probability distributions, densities, return periods and other statistics of the extremes of crest and trough heights as functions of significant wave height.

Keywords: Extreme wave statistics; Wave height; Crest height; Trough height; Generalised Pareto distribution; Extreme value distribution; Return periods

1. Introduction

The most extreme waves in any sea state are of great interest to the oceanographic community. It is these waves that are responsible for the most extreme loadings on ocean vessels and offshore structures. It is important, therefore, that, during the design process, navel architects and engineers use statistical models of the relative occurrence of these potentially dangerous events that are as accurate as possible given the current state of knowledge of these phenomena. This paper provides statistical models for the relative

* Fax: +44 131 451 5078.
E-mail address: p.stansell@ed.ac.uk.

0029-8018/$ - see front matter © 2004 Elsevier Ltd. All rights reserved.
doi:10.1016/j.oceaneng.2004.10.016

occurrence of the most extreme wave, crest and trough heights measured during severe storm conditions in deep water.

The term 'freak wave' is frequently used in the literature and is commonly defined as a wave for which the crest-to-trough wave height is more than twice the value of the significant wave height of the wave record from which it is measured. Thus, a wave is a freak wave if $H^* > 2H^*_{1/3}$, where H^* is the zero-crossing wave height and $H^*_{1/3}$ is the significant wave height (which is defined as the mean of the highest third of the waves in the record). Note that dimensional height measures are denoted with a superscripted asterisk (*) to differentiate them from dimensionless height measures which are introduced later and denoted without a superscripted asterisk.

In this study, we examine 795 h of wave records measured during periods of severe storms in the North Sea. This data sample, which is described in detail in Section 2, contains some 354,000 individual waves and 104 freak waves.

The common expectation is that the Rayleigh distribution *over-predicts* the probability of occurrence of large waves (but not necessarily freak waves) when compared with models fitted to field data (Mori et al., 2002; Nerzic and Prevosto, 1997; Massel, 1996; Tayfun, 1990, 1981a,b; Krogstad, 1985; Forristall, 1978; Haring et al., 1976). Two recent studies Mori et al. (2002) and Yasuda and Mori (1997), however, suggest that the Rayleigh distribution tends to *under-predict* the probability of occurrence of freak waves, but detailed statistical models are not given. In a previous paper by the author (Stansell, 2004), it was shown (using data which is identical to that used in this study) that, the probability of occurrence of freak waves was severely under-predicted by the Rayleigh distribution. It was shown that the Rayleigh distribution over-predicted the return period of the most extreme freak wave in the data by about 300 times when compared to the fitted model.

The same is not true for the probability of occurrence of the largest crest heights as these are expected to be under-predicted by the Rayleigh distribution (Mori et al., 2002; Al-Humoud et al., 2002; Nerzic and Prevosto, 1997). This is confirmed and quantified by the results in this study. To the author's knowledge, a study of the statistics of extreme troughs heights measured from field data has not been published in the literature. As expected from consideration of the high degree of non-linearity of extreme waves, we find that the Rayleigh distribution considerably under-predicts the probability of occurrence of the extreme crest heights, but only slightly over-predicts the probability of occurrence extreme trough heights. A versatile statistical model, particularly suited to modelling the extremes of distributions, is fitted to the empirical wave, crest and trough height data in the tails of these distributions and the fitted parameters are given. From these models, one can estimate probability densities, extreme value densities and return periods for these extremes.

2. The data

The data used in this study are the same as that used and described in Stansell (2004) The raw data were collected from three Thorn EMI infra-red laser altimeters sampling at 5 Hz and mounted on three of the corners of the North Alwyn fixed steel-jacket oil and gas platform. The Alwyn North field, operated by TotalFinaElf, is situated in the northern North Sea about 100 miles east of the Shetland Islands (60°48.5′ North and 1°44.17′ East) in a water depth of approximately 130 m. There are two jacket platforms in close proximity connected by a walkway. The field processing platform, NAA, is the site of all the sensor and data logging equipment. The logging system is configured so that each sensor takes five measurement of the sea surface elevation every second. These are recorded for a duration of 20 min after which the significant wave height for this period, $H^*_{m_0}$, is calculated as four times the square root of the variance of the 20-min record. If $H^*_{m_0}$ is greater than 3 m, all three 20-min sea surface records are saved to optical disk ready for detailed analysis. We define a storm as the period between the start of the first record and the end of the last, of a continues sequence of 20-min records each satisfying $H^*_{m_0} \gtrsim 3$ m.

In this study, we analyse data collected over the full durations of 14 separate severe storm periods. The storms are of varying bandwidth, but all are essentially uni-modal wind-driven seas without significant swell. To ensure the cleanest data, for each storm, we only use data from the altimeter which is upwind of the platform.

The raw data were stored as 2381 20-min records of surface elevation measurements. Note that all wave records are wholly unfiltered: not being smoothed by any means other than that arising from the finite sampling rate, 5 Hz, of the measurement instruments. This rate of sampling is sufficiently high to yield an accurate representation of the sea surface (see Stansell et al. (2002) for a discussion of the effect of sampling rate on the distribution of sampled wave heights). In a preliminary analysis of these individual 20-min records, the mean surface elevation was subtracted from each elevation measurement to give a wave record in units of metres, and denoted by η, which had a mean elevation of zero. From each $\eta(t_i)$ (excluding those for which $|\eta(t_i)| < 0.01$ m), the time of each zero-crossing was estimated by a linear interpolation from its positive and negative bracketing points by

$$t(\eta = 0) = t_i - \frac{\eta(t_i)\delta t}{\eta(t_{i+1}) - \eta(t_i)},$$

where t_i is the time of the ith measurement, and $\delta t = t_{i+1} - t_i$ is the sampling period (equal to 0.2 s). From the set of zero-crossing times, all zero down-crossing waves were identified in these records. The crest and trough heights for each wave were calculated by $H^*_c = \max(\eta(t_i))$ and $H^*_t = -\min(\eta(t_i))$, where t_i ranges over those values of time which lie between the zero down-crossing times of the wave. The wave height is given by $H^* = H^*_c + H^*_t$. The value of $H^*_{1/3}$ is then calculated for each 20-min wave record as the mean of the highest third of the wave heights, H^*, in that record. A more detailed summary of the data from these storms is given in Table 1.

Fig. 1 shows the most extreme wave height ($H^*/H^*_{1/3} = 3.19$), which is also the most extreme crest height ($H^*_c/H^*_{1/3} = 2.46$), and Fig. 2 shows the most extreme trough height ($H^*_t/H^*_{1/3} = 1.42$).

3. Statistical analysis

3.1. Non-dimensionalising wave, crest and trough heights

Throughout this study, we compare distributions fitted to measured data with the predictions of the Rayleigh distribution, and so it is convenient to work in dimensionless

Table 1
Summary statistics for the data used in this study

Storm ID	No. of 20-min records	No. of waves for which $H^* > H^*_{1/3}$	No. of freak waves	Max (H^*) (m)	Max $(H^*/H^*_{1/3})$	Max $(H^*_c/H^*_{1/3})$	Max $(H^*_t/H^*_{1/3})$
23	177	3459	6	21.94	2.08	1.42	1.04
25	111	2295	2	15.88	2.59	1.46	1.12
26	159	3675	4	9.11	2.15	1.40	1.14
27	139	2776	1	15.05	2.40	1.56	1.1
28	144	2986	6	19.51	2.38	2.03	1.09
29	89	1764	12	20.27	2.30	1.86	0.999
90	293	6006	20	23.85	2.65	2.11	1.06
124	173	2975	0	21.14	1.97	1.33	0.994
127	99	1837	2	16.91	2.08	1.36	1.08
132	285	5831	14	13.15	2.3	1.47	1.06
146	91	2023	4	9.15	2.46	1.42	1.42
149	390	6911	25	24.19	2.50	1.87	1.08
172	158	3079	8	21.32	3.19	2.46	1.06
195	73	1347	0	18.72	1.95	1.22	0.973
Combined	2381	46,964	104	24.19	3.19	2.46	1.42

units. Following Stansell (2004), we define the dimensionless wave height by

$$H = \frac{H^*}{H^*_{1/3}}. \tag{1}$$

Thus, a freak wave is defined as a wave for which $H > 2$. When cast in these dimensionless units the Rayleigh distribution becomes

$$F_R(H) = 1 - \exp\left(-\frac{H^2}{a}\right), \tag{2}$$

and the probability density is given by

$$f_R(H) = \frac{2H}{a}\exp\left(-\frac{H^2}{a}\right), \tag{3}$$

where the value[1] $a = 0.498926$ gives $H_{1/3} = 1$.

It was shown by Stansell (2004) that the distribution of H is, to a good approximation, independent of $H^*_{1/3}$ for the full range $2.5 < H^*_{1/3} < 12.6$ of the data. This allowed the grouping together of all dimensionless wave height data to give a single statistical sample, and therefore circumvented problems associated with the non-stationarity of H^*.

[1] The parameter a is obtained by solution of $\int_{a \ln 3}^{\infty} H f_R(H; a) = \frac{1}{3}$ which gives

$$a = 4(3\sqrt{\pi}(\mathrm{erf}(\sqrt{\ln 3}) - 1) - 2\sqrt{\ln 3})^{-2}.$$

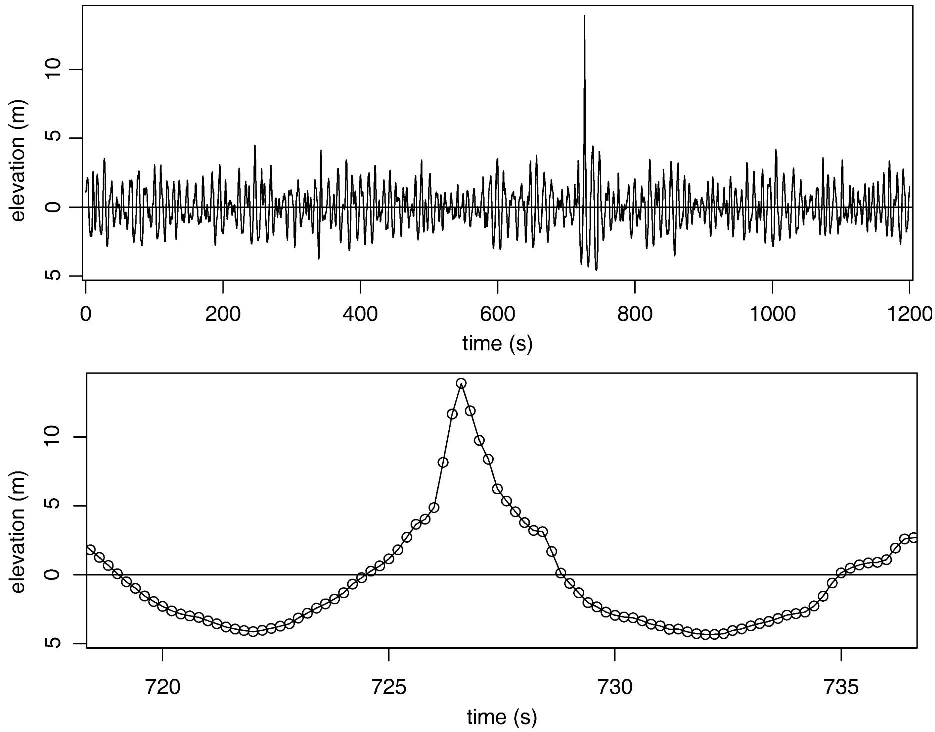

Fig. 1. The most extreme freak wave, which is also the most extreme wave crest, shown in context of the 20-min record, and in detail. This wave is from Storm 172 and has $H_c^* = 13.90$ m, $H_t^* = 4.14$ m, $H_{1/3}^* = 5.65$ m, giving $H^* = 18.04$ m, $H^*/H_{1/3}^* = 3.19$ and $H_c^*/H_{1/3}^* = 2.46$. The zero-crossing period is 9.8 s.

Unfortunately this is not the case for the crest and trough heights. Performing a similar scaling for the crest and trough heights according to

$$H_c = \frac{H_c^*}{H_{1/3}^*}, \tag{4}$$

$$H_t = \frac{H_t^*}{H_{1/3}^*}, \tag{5}$$

shows the dimensionless crest and trough heights, H_c and H_t, have a far weaker dependency than H_c^* and H_t^* on $H_{1/3}^*$, but, unlike H, the dependency of H_c and H_t is considered strong enough to warrant their subgrouping based on associated values of $H_{1/3}^*$. This is demonstrated graphically as follows.

The data are sorted into 20 equally sized groups according to their values of $H_{1/3}^*$ For each of these groups Fig. 3 shows sets of probability quantiles for the dimensional variables H^*, H_c^* and H_t^* compared with those for the dimensionless variables H, H_c and

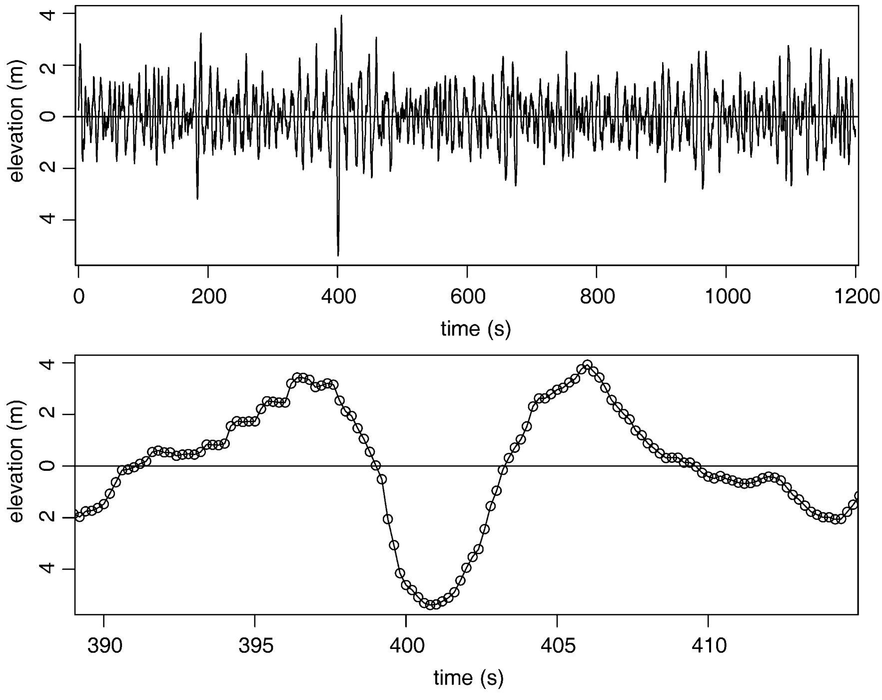

Fig. 2. The most extreme wave trough shown in context of the 20-min record, and in detail. This wave is from Storm 146 and has $H_c^* = 13.92$ m, $H_t^* = 5.38$ m and $H_{1/3}^* = 3.79$ m, giving $H^* = 9.31$ m and $H_t^*/H_{1/3}^* = 1.42$. The zero-crossing period is 10.11 s.

H_t. These quantiles correspond to the nine probability levels $p = \{0.1, 0.3, 0.5, 0.7, 0.8, 0.9, 0.95, 0.99, 0.999\}$. For each probability level the quantiles are connected across groups to obtain a series of probability contours. Also shown are connecting lines given by a *locfit* local regression[2] with the 95% confidence bands. In each case, strong dependency of the dimensional variables is observed, and a week dependency of the non-dimensionalised variables. The variation of H over the full range of $2.5 < H_{1/3}^* < 12.6$ is about 10%, and Stansell (2004) judged that this variation was sufficiently small to avoid the need to group the data based on values of $H_{1/3}^*$. The plots in Fig. 3 show that the variations in both H_c and H_t are larger. The variation in the $p = 0.999$ probability contour for H_c against $H_{1/3}^*$ is about 42% over the full range $H_{1/3}^*$, and that for H_t is about 24%. It is judged here, therefore, that

[2] This is a non-parametric local regression procedure called *locfit* (Loader, 1999). For each value of a predictor variable, x, locfit estimates the response variable, y, as $y = f(x) + \varepsilon$, where $f(x)$ is a non-parametric function obtained by a local regression for those observations in the neighbourhood of x, and ε is a residual random variable. One advantage of using a non-parametric regression is that it is not required to specify, a priori, the functional form of $f(x)$. In particular, the locfit algorithm is very flexible, making it ideal for modelling complex processes for which no theoretical models exist.

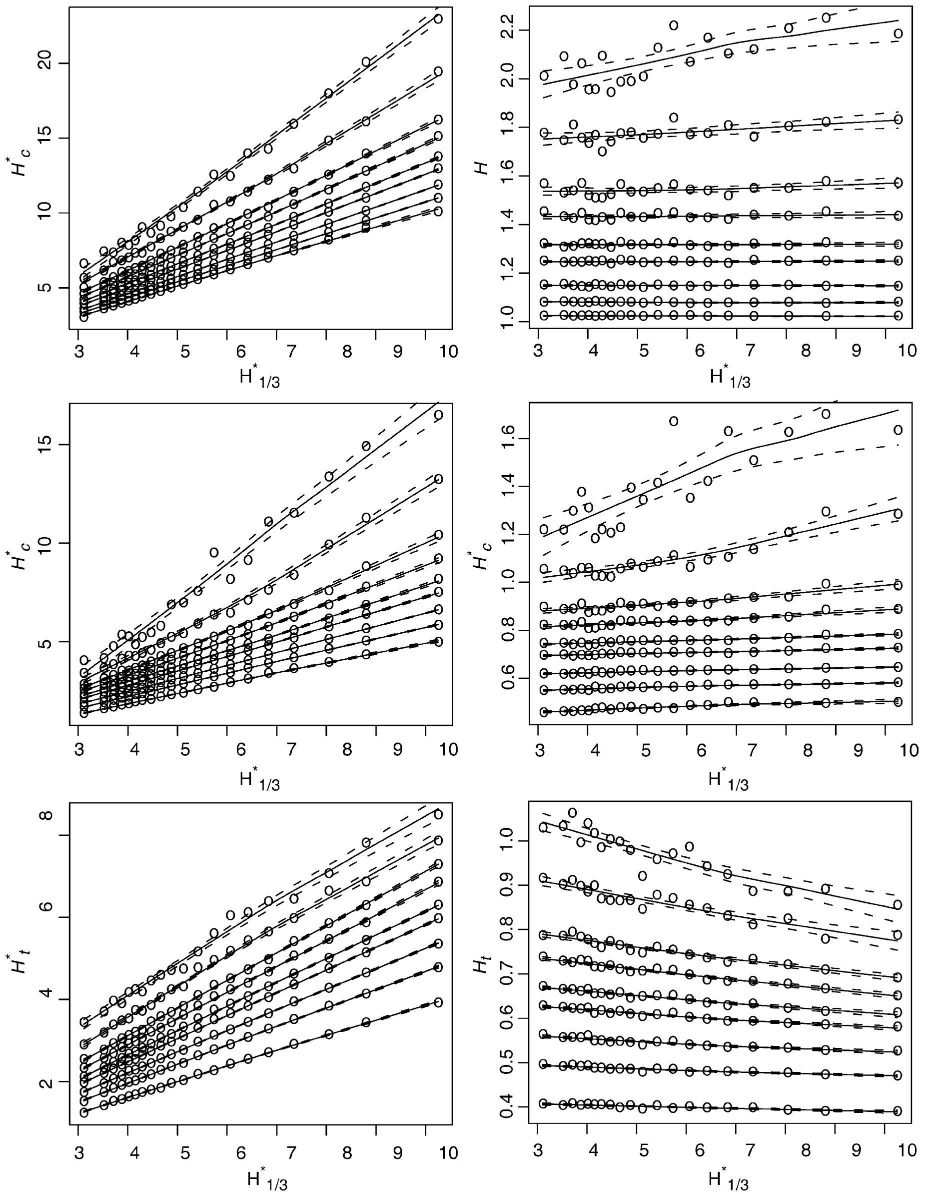

Fig. 3. Probability contours (with 95% confidence bands) showing the dependency of dimensional and dimensionless of crest and trough height on $H^*_{1/3}$.

the variation in H_c and H_t is large enough to warrant grouping these data based on values of $H^*_{1/3}$.

In the following, we partition the data into five groups based on the values of $H^*_{1/3}$. Within each group the variables H_c and H_t are assumed to be sufficiently stationary to

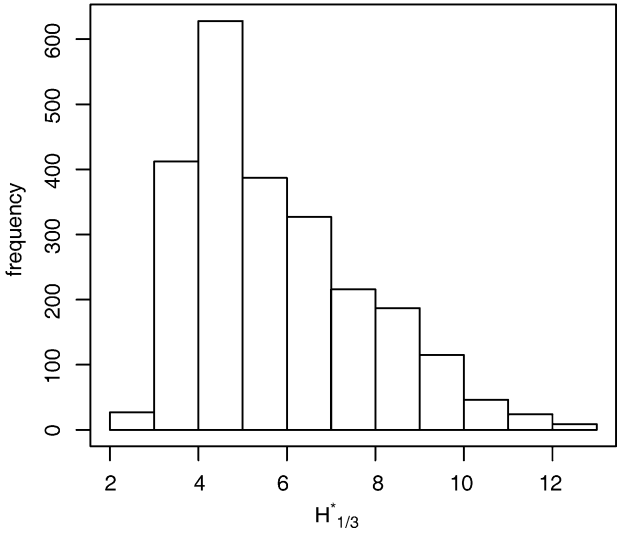

Fig. 4. Histogram of $H^*_{1/3}$ in our data.

apply statistical analyses which require this condition. A parallel analysis is carried out for grouped values of H for completeness. The advantage of using suitably non-dimensionalised measures of the data is that it greatly increases the size of the statistical samples in each group and therefore reduces any statistical errors. A histogram of the values of $H^*_{1/3}$ from the 20-min records of our data is show in Fig. 4. The mean of $H^*_{1/3}$ from all the data is $\bar{H}^*_{1/3}=5.53$.

3.2. Distributions of largest waves, crests and troughs

Asymptotic theory (Embrechts et al., 1997; Coles, 2001) suggests that for large enough threshold, u, the distribution function of a stationary random variable X is approximated by a *generalised Pareto distribution* (GPD). This has the distribution function

$$F_{\xi\mu\sigma}(x) = 1 - \bar{F}_{\xi\mu\sigma}(x) \tag{6}$$

where the complementary distribution function is given by

$$\bar{F}_{\xi\mu\sigma}(x) = \begin{cases} \left(1+\frac{\xi(x-\mu)}{\sigma}\right)^{-1/\xi} & \text{if } \xi \neq 0, \\ \exp\left(-\dfrac{x-\mu}{\sigma}\right) & \text{if } \xi = 0, \end{cases} \tag{7}$$

and where

$$x \geq \mu \text{ if } \xi \geq 0, \quad \mu \leq x \leq \mu - \sigma/\xi \text{ if } \xi < 0.$$

Here ξ, μ and $\sigma > 0$ are, respectively, shape, location and scale parameters for the GPD. (Note in particular that $\bar{F}_{\xi\mu\sigma}(x)$ is continuous in ξ at $\xi=0$.)

In order to estimate the distribution of the largest observations of X, the following GPD model for the tail of the distribution is fitted

$$\Pr(X > x) = \bar{F}_{\xi\mu\sigma}(x), \tag{8}$$

valid for all x greater than or equal to some appropriately chosen threshold u.

Elementary calculation shows that

$$\Pr(X > u + x | X > u) = \frac{\bar{F}_{\xi\mu\sigma}(u + x)}{\bar{F}_{\xi\mu\sigma}(u)}, \tag{9}$$

$$\Pr(X > u + x | X > u) = \bar{F}_{\xi 0 \tilde{\sigma}}(x), \tag{10}$$

where for both $\xi = 0$ and $\xi \neq 0$

$$\tilde{\sigma} = \sigma + \xi(u - \mu). \tag{11}$$

Thus, for sufficiently large u, asymptotic theory (Embrechts et al., 1997; Coles, 2001) suggests that the distribution function of the excess $x = (X - u)$ is approximated by a GPD parameterised by ξ, which is threshold independent, and $\tilde{\sigma}$, which is threshold dependent. The parameters ξ and $\tilde{\sigma}$ were determined by maximum likelihood estimation based on all values of X greater than u. We recorded whether or not X exceeded the threshold u and, if so, the value of its excess $x = (X - u)$. The values of the excesses are sufficient for the estimation of ξ and $\tilde{\sigma}$.

The values of the original (threshold independent) parameters μ and σ may now be recovered. Letting p denote the probability that X is greater than u, one can write, under the model (8)

$$p = \Pr(X > u) = \bar{F}_{\xi\mu\sigma}(u). \tag{12}$$

The number of observations exceeding u is sufficient for the estimation of p, and μ and σ may then be recovered via the relations (7), (11) and (12). Thus, for all ξ

$$\sigma = \tilde{\sigma} p^{\xi}, \tag{13}$$

$$\mu = u + \frac{\tilde{\sigma}}{\xi}(p^{\xi} - 1), \tag{14}$$

and, in particular, for $\xi = 0$

$$\sigma = \tilde{\sigma}, \tag{15}$$

$$\mu = u + \tilde{\sigma} \ln p. \tag{16}$$

Analysis of the grouped data in this study suggests that there is insufficient data in each group for a GPD to convincingly represent the asymptotic limit of the distributions. Thus, we have chosen to avoid estimating an appropriate value for the threshold, and instead we fitted the GPD model (8), with X equal to one of the dimensionless variables H, H_c or H_t, to the 100 most extreme observations in each data group. It is important to note that, assuming convergence has not been reached, the fitted GPD models should not be extrapolated beyond the largest measured observation used in the fit. In this

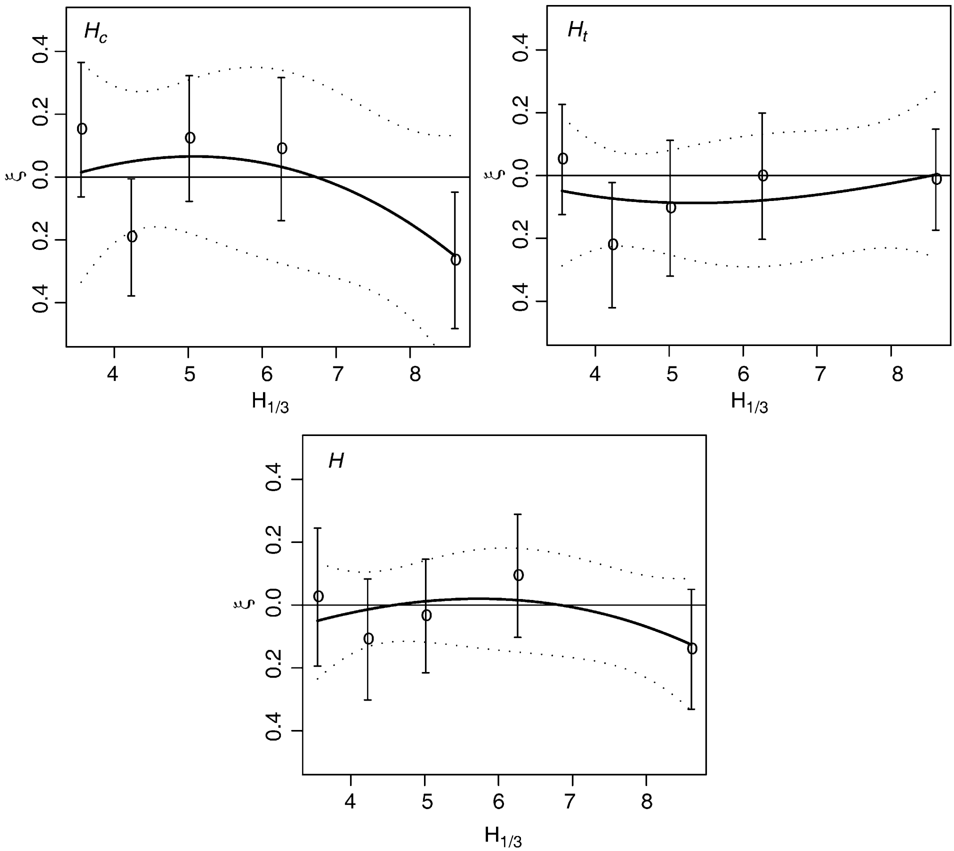

Fig. 5. Fitted shape parameter, ξ, for the GPD models of H, H_c and H_t as functions of $H^*_{1/3}$ over the five data groups.

case, the interpretation of the results should be that the family of GPDs is a sufficiently large and flexible class for the purpose of interpolating the distributions of the data we have.

The values of the thresholds and fitted parameters are given in Table A1 of Appendix A.[3] For comparison and in the same appendix, Table A2 shows the fitted parameters for the case that all the data was grouped into one statistical sample. In these tables, $\bar{H}^*_{1/3}$ denotes the mean of $H^*_{1/3}$ calculated over the data group. Figs. B1 and B2 in Appendix B show quantile–quantile plots of the empirical and fitted distributions for X above the thresholds, u, for the fitted parameters given in Tables A1 and A2, respectively.

Fig. 5 shows plots of the shape parameter, ξ for the GPD fits of H, H_c and H_t as functions of $\bar{H}^*_{1/3}$ over the five data groups, along with error bars which extend to plus

[3] The *S-Plus* code from Coles (2001) was used to obtain these fits.

and minus twice the standard errors on the fitted values. Also shown is a *locfit* local regression of ξ against $\bar{H}^*_{1/3}$ with 95% confidence bands. Notice that the standard errors on ξ are about the same magnitude as the values of ξ themselves. This fact, together with the plots in Fig. 5, presents no convincing evidence that $\xi \neq 0$ for any of the fits of grouped data. Indeed, it may be argued that choosing $\xi = 0$ in all instances is as well-founded as using the values fitted, although in the following analysis the actual fitted values are used.

Fig. 6 shows plots of location parameter or threshold, u, and fitted scale parameter, $\tilde{\sigma}$, for the GPD fits of H, H_c and H_t as functions of $\bar{H}^*_{1/3}$ over the five data groups. Also shown is a locfit local regressions of u and $\tilde{\sigma}$ and against $\bar{H}^*_{1/3}$ with 95% confidence bands. As expected, we see that u for the GPD models of H is approximately constant, while that for H_c increases, and that for H_t decreases, with increasing $\bar{H}^*_{1/3}$. We also see that $\tilde{\sigma}$ increase for the models of both H and H_c with increasing $\bar{H}^*_{1/3}$, but decrease for those of H_t.

3.3. Comparison of fitted GPD with Rayleigh distributions

We now examine the differences between the predictions of the Rayleigh probability density function and those of the GPD. The GPD densities are defined by $f_{\xi\mu\sigma}(x) = \mathrm{d}F_{\xi\mu\sigma}(\mathrm{x})/\mathrm{d}x$, and can be written in terms of the threshold independent parameters as

$$f_{\xi\mu\sigma}(x) = \begin{cases} \dfrac{1}{\sigma}\left(1 + \dfrac{\xi(x-\mu)}{\sigma}\right)^{-(1+\xi)/\xi} & \text{if } \xi \neq 0, \\ \dfrac{1}{\sigma}\exp\left(-\dfrac{x-\mu}{\sigma}\right) & \text{if } \xi = 0, \end{cases} \tag{17}$$

or, in terms of the threshold dependent parameters, as

$$f_{\xi 0\tilde{\sigma}}(x) = \begin{cases} \dfrac{p}{\tilde{\sigma}}(1 + \xi x\tilde{\sigma})^{-(1+\xi)/\xi} & \text{if } \xi \neq 0, \\ \dfrac{p}{\tilde{\sigma}}\exp(-x\tilde{\sigma}) & \text{if } \xi = 0. \end{cases} \tag{18}$$

The distribution of the largest value that is expected to occur in a certain number, n, of observations is called the extreme value distribution. The extreme value distribution is given in terms of the parent distribution, $F(x)$, by $G(x;\, n) = \Pr(X_n < x) = F^n(x)$ and the corresponding extreme value density is given by $g(x;\, n) = \mathrm{d}F^n(x)/\mathrm{d}x = n\,f(x)F^{n-1}(x)$. If the tail of the parent distribution is Rayleigh distributed then the density function for the extreme value obtained from n measurements (that is, n waves) is given by

$$g_{\mathrm{R}}(x; n) = nf_{\mathrm{R}}(x)F_{\mathrm{R}}^{n-1}(x), \tag{19}$$

where $F_{\mathrm{R}}(x)$ and $f_{\mathrm{R}}(x)$ are given by Eqs. (2) and (3). If the tail of the distribution is a GPD then the density function for the extreme value is given by

$$g_{\xi\mu\sigma}(x; n) = nf_{\xi\mu\sigma}(x)F_{\xi\mu\sigma}^{n-1}(x), \tag{20}$$

where $F_{\xi\mu\sigma}(x)$ and $f_{\xi\mu\sigma}(x)$ are given by Eqs. (6), (7) and (17).

Fig. 7 shows plots of the Rayleigh density compared with the fitted GPD models for each of the five data groups and each of the variables $X = \{H, H_c, H_t\}$, and also for the case

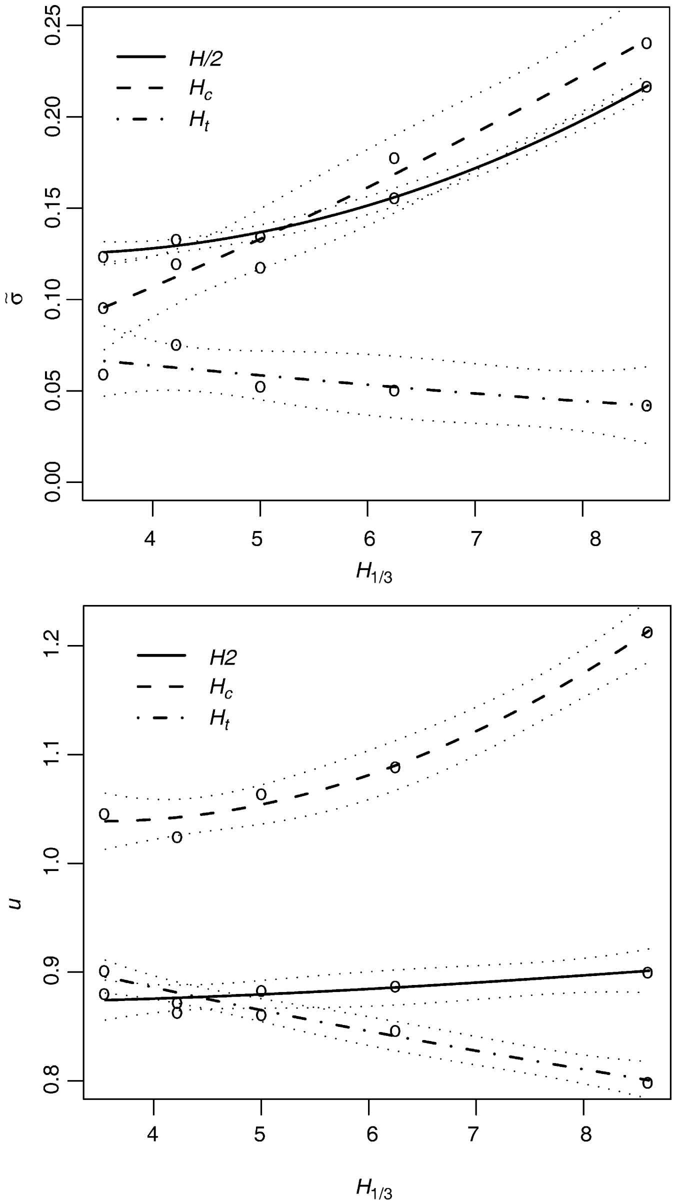

Fig. 6. Fitted location parameter or threshold, u, and scale parameter, $\tilde{\sigma}$, for the GPD models of H, H_{c} and H_{t} as functions of $H^{*}_{1/3}$ over the five data groups.

that all the data are grouped together. The GPD models are plotted only within the range of the data to which the model was fitted. In this way, no extrapolation is made.

The need to group the H_{c} and H_{t} data is confirmed in these plots as the order of the fitted GPD models agrees with the expected order based on the order of the means

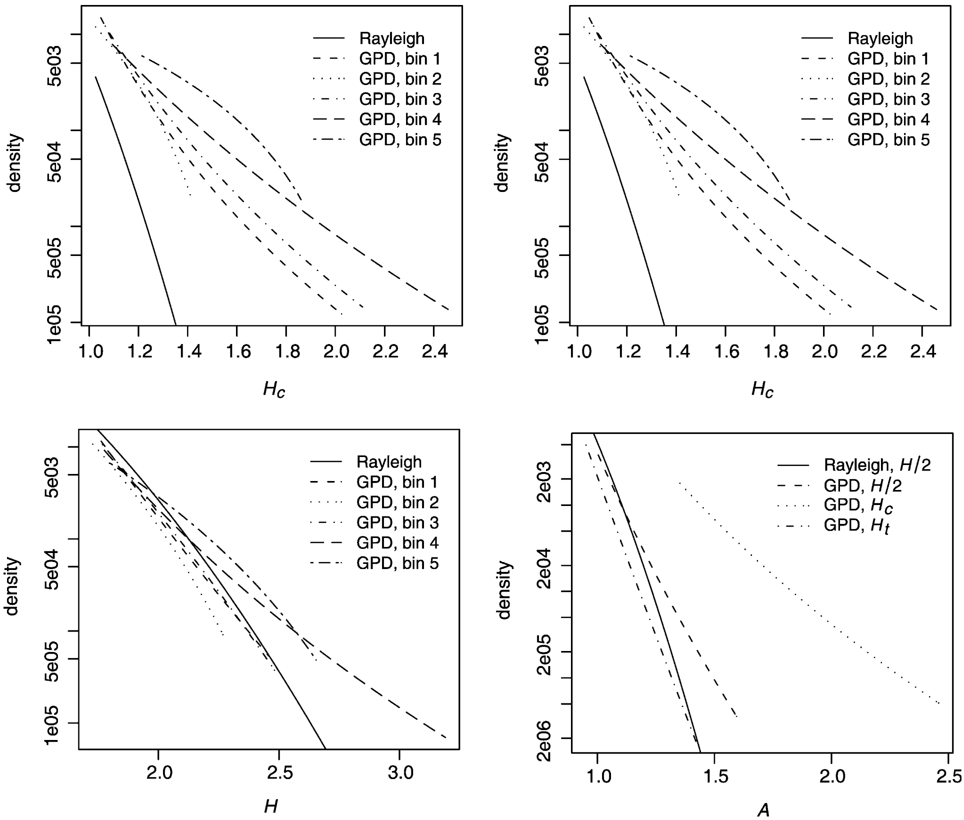

Fig. 7. Probability densities predicted from the Rayleigh distribution and those obtained from the fitted GPD models for the 100 most extreme wave, crest and trough heights measured from grouped and ungrouped data.

of $H^*_{1/3}$ in these groups. For example, bin 5 of H_c contains the data with the highest mean value of $H^*_{1/3}$ and the GPD fitted to these data give the largest predicted density of large values of H_c; also the bins with the lowest values of the mean of $H^*_{1/3}$ are bins 1 and 2 and the fits to these data give the lowest predicted densities for large values of H_c. The expected bin order, from the lowest to highest probability, is also shown in the fitted GPDs for H_t. That grouping is not required for the H data is supported by the observation that the spread in the fitted GPDs is small, and the order from highest to lowest probability is not observed. (Although it does appear that the Rayleigh distribution over-predicts the probability of occurrence of the most extreme values of H in the three data groups with lowest $H^*_{1/3}$, and it under-predicts the probability of occurrence of the most extreme values of H in the two data groups with largest $H^*_{1/3}$).

Fig. 8 shows comparisons of the predictions of Eqs. (19) and (20) with $n = 70{,}000$, which is approximately equal to one fifth of the total number of waves in our data

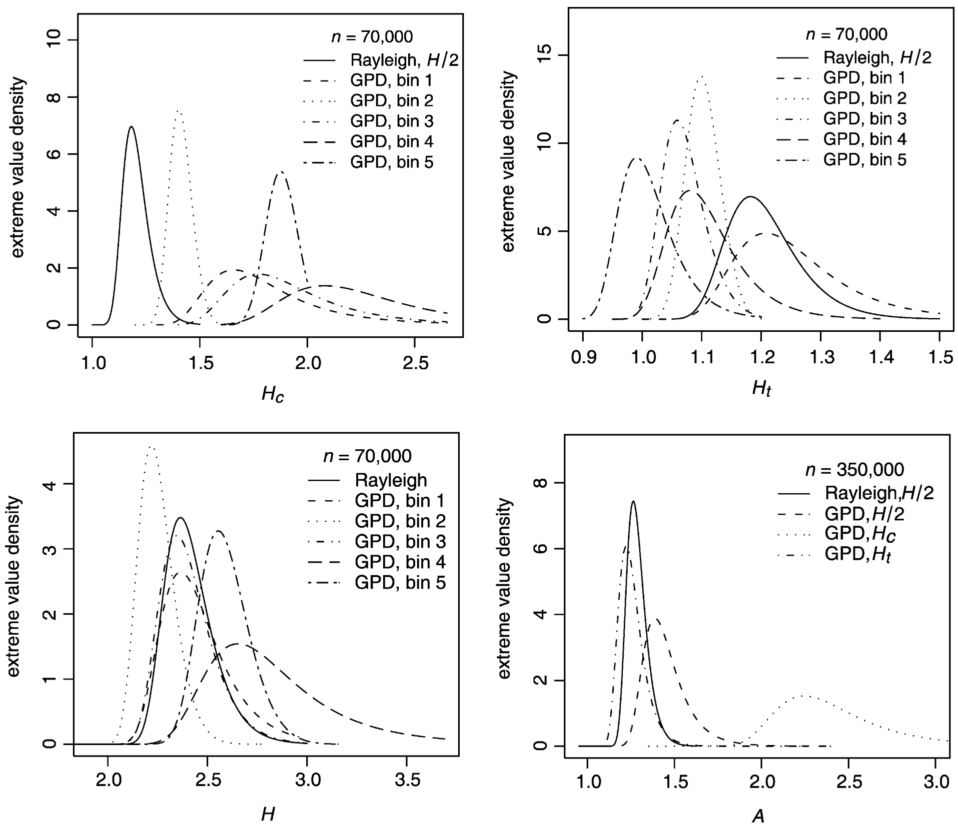

Fig. 8. Comparisons of extreme value densities predicted from the Rayleigh distribution and those obtained from the fitted GPD models for the 100 most extreme wave, crest and trough heights measured from grouped and ungrouped data.

sample. Also shown are plots of extreme value densities obtained from fitted GPDs for the case, with $n = 350{,}000$, that all the data were grouped together. Any errors in the fitted GPDs are magnified in the corresponding extreme value densities. Even so, from the plots of the extreme value densities for H_c in Fig. 8 we see that the fitted bin order from the lowest to highest probability is 2, 1, 3, 5, 4 instead of the expected bin order of 1, 2, 3, 4, 5 (based on the position of the mode of the distribution). Also, the plot for bin 5 appears erroneous as it has too sharp a cut-off in the upper limit of the data. For the case of H_t the order of the fitted bins is as expected except for bins 3 and 4 being exchanged. From the plots of the extreme value densities for H, we see that the fitted group (or bin) order from the lowest to highest probability is 4, 5, 1, 3 and 2, which, as before, shows no strong ordering dependent on the mean values of $H^*_{1/3}$ associated with the data groups.

The last plot in Fig. 8, which shows the fits obtained when all the data are grouped together, strongly supports the expectation that the extreme value density for trough

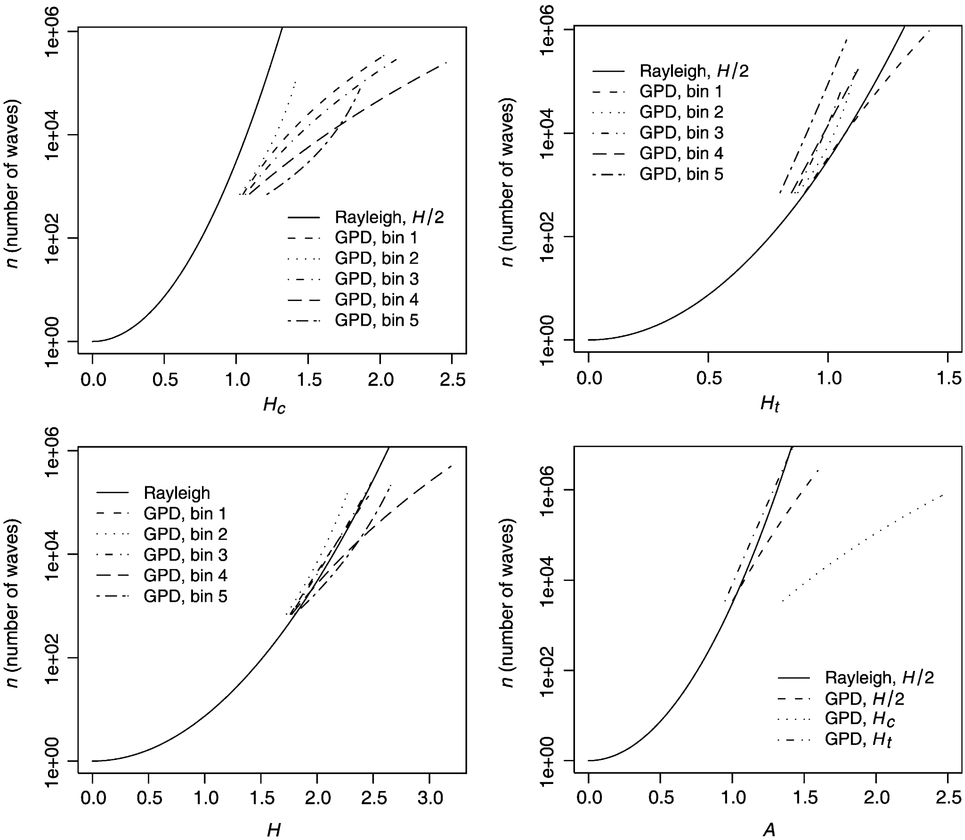

Fig. 9. Comparisons of return periods predicted from the Rayleigh distribution and those obtained from the fitted GPD models for the 100 most extreme wave, crest and trough heights measured from grouped and ungrouped data.

heights is over-predicted, and that for crest heights is under-predicted, by the Rayleigh density. It also shows that the extreme value density for wave heights is under-predicted by the Rayleigh density. The degree of these over and under predictions is quantified by the parameters fitted to the GPD models and given in Tables A1 and A2.

Fig. 9 shows the return periods (in units of the number of waves and defined by $1/(1-F(H))$) predicted form the Rayleigh model compared with those from the GPDs models fitted to the data. The graphs for the fitted GPDs are plotted only over the range of the data to which the models were fitted so that no extrapolation is made.

Table 2 presents the ratios of return periods predicted from the Raleigh distribution and the fitted GPD models. Values are presented for the minimum freak wave heights and for the most extreme wave, crest and trough heights observed in our data.

Table 2
Ratios of return periods predicted from the Rayleigh distribution and the fitted GPD models for the minimum freak wave heights and the most extreme wave, crest and trough heights observed in our data

Variable $X=x$	Ratio of return periods, $\bar{F}_R(x)/\bar{F}_{\xi\mu\sigma}(x)$
$H=2$	0.91
$H_c=1$	10.0
$H_t=1$	0.38
$H=3.19$	270
$H_c=2.46$	1.55×10^{15}
$H_t=1.42$	1.22

For the minimum freak wave height of $H=2$ the return periods from the Rayleigh and fitted GPD models are about the same; for the minimum freak wave crest height of $H_c=1$, the Rayleigh distribution under-predicts the return period when compared with the fitted GPD model (note that this prediction required extrapolation of the GPD); and, for the minimum freak wave trough height of $H_t=1$ the Rayleigh distribution over-predicts the return period when compared with the fitted GPD model. For the most extreme freak wave height of $H=3.19$, the Rayleigh distribution severely under-predicts the return period when compared to the fitted GPD model; for the most extreme wave crest height of $H_c=2.46$, the Rayleigh model hopelessly under-predicts the return period when compared with the fitted GPD model; and, for the most extreme wave trough height of $H_t=1.42$, the return periods from the Rayleigh and fitted GPD models are about the same.

4. Discussion

Based on the analysis presented here, it is the author's opinion that the partitioned data groups do not contain enough observations for the GPDs to have converged to their asymptotic forms. If this is correct, the interpretation of the results should be that the family of GPDs is a sufficiently large and flexible class for the purpose of modelling and interpolating the distributions of the data we have. It would, therefore, be unwise to extrapolate the fitted distributions far beyond of the range of the data to which the models were fitted. Indeed, we believe that at least five times as many observations would be needed for the fitted GPD models to approach their asymptotic forms. Thus, the GPDs fitted to the grouped H_c and H_t data have probably not converged, whereas that fitted to the ungrouped H data may have.

As expected, the fitted GPDs show that the Rayleigh distribution is not suitable for modelling the probability of occurrence of extremes of H_c or H_t. Adjustments to the Rayleigh distribution to account for second-order nonlinear corrections given by Tung and Huang (1985) do not significantly improve the predictions, and indeed, they give worse predictions than the Rayleigh distribution for large wave troughs.

It is the considered opinion of the author that an acceptable approach, which may be used to estimate the density of extreme crest and trough heights as functions of $H^*_{1/3}$ in cases where a better or more reliable alternative is unavailable, is as follows:

(1) Read off the values of u and $\tilde{\sigma}$ from the local regressions presented in Fig. 6.
(2) Set $\xi=0$ (in accordance with Fig. 5) and then calculate μ and σ from Eqs. (15) and (16) with $p=0.001434$ (from Table A1).
(3) Use these values of μ and σ to estimate $\bar{F}_{0\mu\sigma}(x)$ and $f_{0\mu\sigma}(x)$ in the $\xi=0$ expressions from Eqs. (7) and (17), respectively.

These estimated densities and distributions should not be used below their appropriate threshold, u. Also, care should be taken when applying them at the high height limits observed in the data. This is because, as previously stated, we are not confident that the GPDs have converged to their asymptotic forms. Indeed, although one would always expect some wander in extremes of qq-plots of the fitted models, the qq-plots in Fig. B1 show, in all but one case, that the models fitted to grouped data are under-predicting the probability of occurrence of the most extreme values in the data.

Note that, because the locate regressions in Fig 5 and 6 aid in smoothing the noisy statistical data and uncovering the fundamental relation between the predictor variable, $H^*_{1/3}$, and the response variable, H_c or H_t, it is expected that this procedure has the advantage of providing fitted models with less statistical error (as seen in Figs. 7–9) than the models based on grouped data alone.

5. Conclusions

GPD models have been fitted to empirical data to give estimates of the probability of occurrence of the most extreme wave, crest and trough heights in wind-driven, broad-banded, severe storm seas. Fitted parameter values for these statistical models are tabulated for the cases of the GPD being fitted to the 100 most extreme observation from each of five datasets grouped by $H^*_{1/3}$, and also for the cases that all data were combined into a single dataset independent of $H^*_{1/3}$. The fitted GPDs show, as expected, that the Rayleigh distribution is inadequate for modelling the probability of occurrence of extremes of H_c or H_t, but, more importantly, they provide actual parametric models which may be used during the design process to obtain more realistic and accurate predictions of the extremes of given sea states if a better or more reliable alternative is unavailable. By the procedure presented in Section 4, one may acquire estimates of the probability distributions, densities, return periods and other statistics of extremes of crest and trough heights as functions of significant wave height. These estimates should be used with caution as it is the author's opinion that the partitioned data groups for H_c and H_t do not contain enough observations for the GPDs to have converged to their asymptotic forms. The estimated distributions therefore represent models fitted to the data, and not the limiting asymptotic forms of the distributions. It would, therefore, be unwise to extrapolate the fitted distributions far beyond of the range of the data to which the models were fitted.

Appendix A. Tables of fitted GPD parameters

Tables A1 and A2 present the parameters values fitted to the GPD models for the 100 most extreme values of each of $X={H, H_{c},H_{t}}$ when split in to five groups depending on the values of $H_{1/3}^{*}$, and when all the data is combined into a single data set.

Table A1
Thresholds and fitted parameters for GPDs fitted to the 100 most extreme observations from each of data group

X	Bin	$\bar{H}^*_{1/3}$	u	$\tilde{\sigma}\pm$SE	$\xi\pm$SE	p	σ	μ
H_c	1	3.55	1.046	0.0959 ± 0.0140	0.1509 ± 0.1070	0.001434	0.0357	0.6477
	2	4.23	1.025	0.1200 ± 0.0162	-0.1920 ± 0.0932	"	0.4218	-0.5467
	3	5.01	1.065	0.1181 ± 0.0166	0.1225 ± 0.0999	"	0.0530	0.5330
	4	6.26	1.089	0.1780 ± 0.0269	0.0888 ± 0.1138	"	0.0995	0.2055
	5	8.61	1.214	0.2410 ± 0.0350	-0.2652 ± 0.1085	0.001435	1.3680	-3.0350
H_t	1	3.55	0.902	0.0596 ± 0.0079	0.0511 ± 0.0876	0.001434	0.0426	0.5707
	2	4.23	0.873	0.0759 ± 0.0106	-0.2213 ± 0.0997	"	0.3229	-0.2439
	3	5.01	0.862	0.0529 ± 0.0078	-0.1040 ± 0.1080	"	0.1045	0.3653
	4	6.26	0.847	0.0508 ± 0.0072	-0.0022 ± 0.1006	"	0.0516	0.5118
	5	8.61	0.799	0.0426 ± 0.0054	-0.0130 ± 0.0803	0.001435	0.0463	0.5086
H	1	3.55	1.762	0.1240 ± 0.0184	0.0252 ± 0.1098	0.001434	0.1052	1.0130
	2	4.23	1.727	0.1334 ± 0.0185	-0.1095 ± 0.0963	"	0.2731	0.4508
	3	5.01	1.768	0.1350 ± 0.0182	-0.0349 ± 0.0904	"	0.1696	0.7749
	4	6.26	1.776	0.1561 ± 0.0218	0.0930 ± 0.0978	"	0.0850	1.0100
	5	8.61	1.801	0.2171 ± 0.0298	-0.1408 ± 0.0952	0.001435	0.5459	-0.5331

For the threshold dependent parameters standard errors are included.

Table A2
Thresholds and fitted parameters for GPDs fitted to the 100 most extreme observations from all data bins combined

X	$\bar{H}^*_{1/3}$	U	$\tilde{\sigma}\pm$SE	$\xi\pm$SE	p	σ	μ
H_c	5.53	1.353	0.160 ± 0.026	0.090 ± 0.127	0.0002869	0.303	-0.745
H_t	"	0.951	0.058 ± 0.007	0.009 ± 0.073	"	0.054	0.495
H	"	2.006	0.150 ± 0.021	0.050 ± 0.094	"	0.026	1.574

For the threshold dependent parameters standard errors are included.

Appendix B. Quantile–quantile plots

Figs. B1 and B2 show quantile–quantile plots comparing the empirical and fitted distributions for the 100 most extreme values of each of $X=\{H, H_c, H_t\}$ when split in to five groups depending on the values of $H^*_{1/3}$ and when all the data is combined into a single data set. The fitted parameters are given in Tables A1 and A2, respectively.

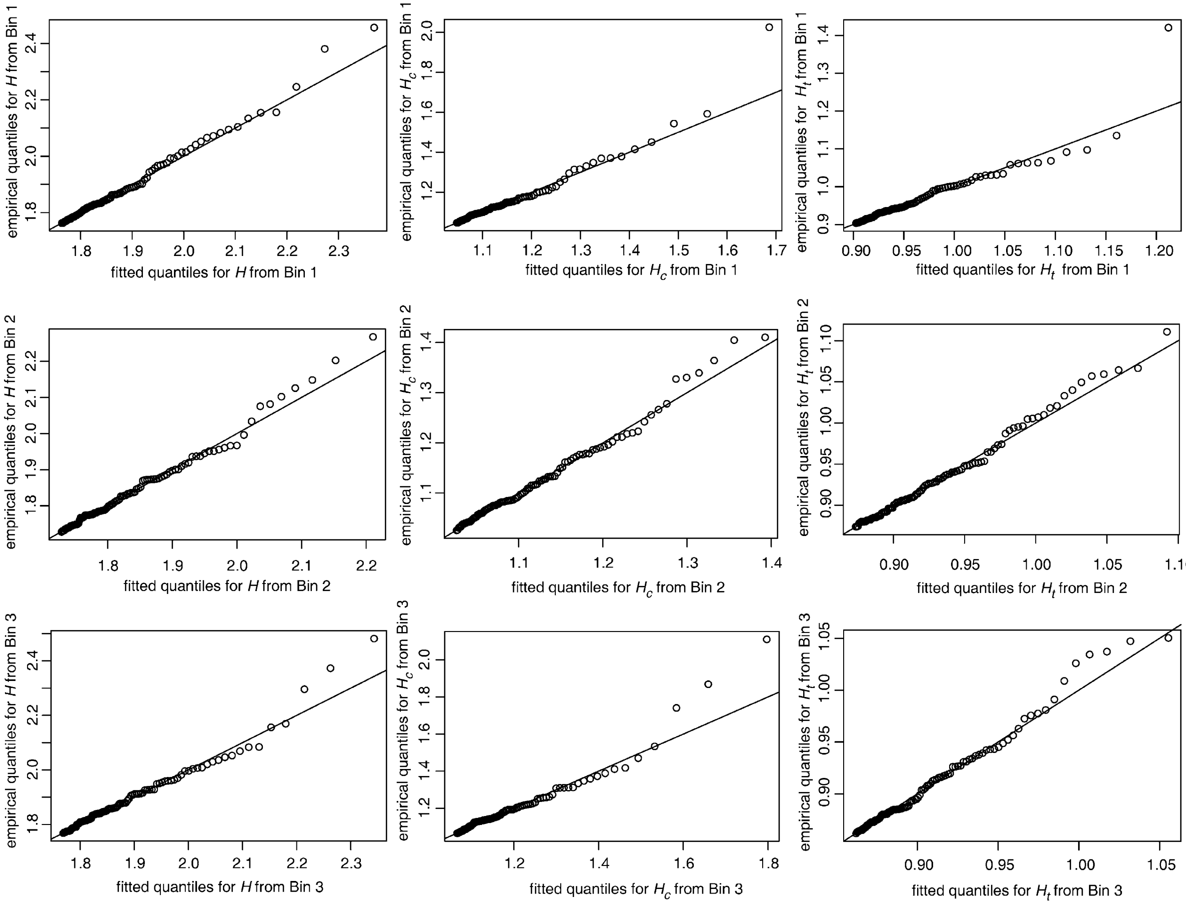

Fig. B1. Quantile–quantile plots of empirical distributions and GPD fits for grouped dimensionless wave, crest and trough heights.

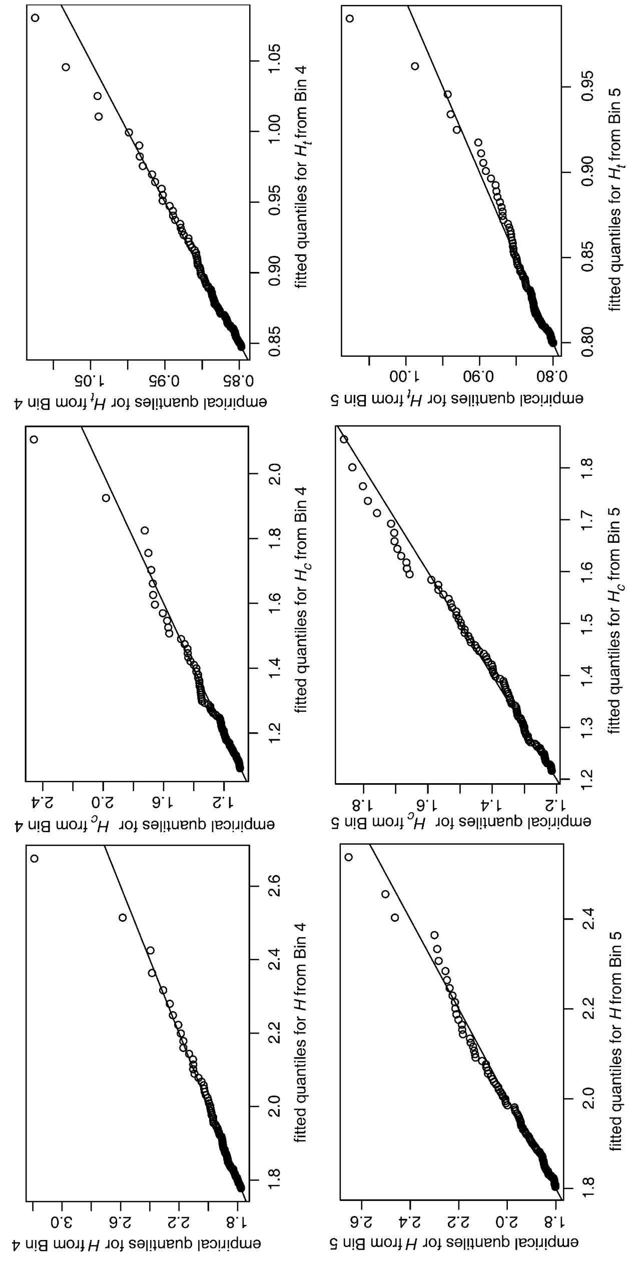

Fig. B1 (*continued*)

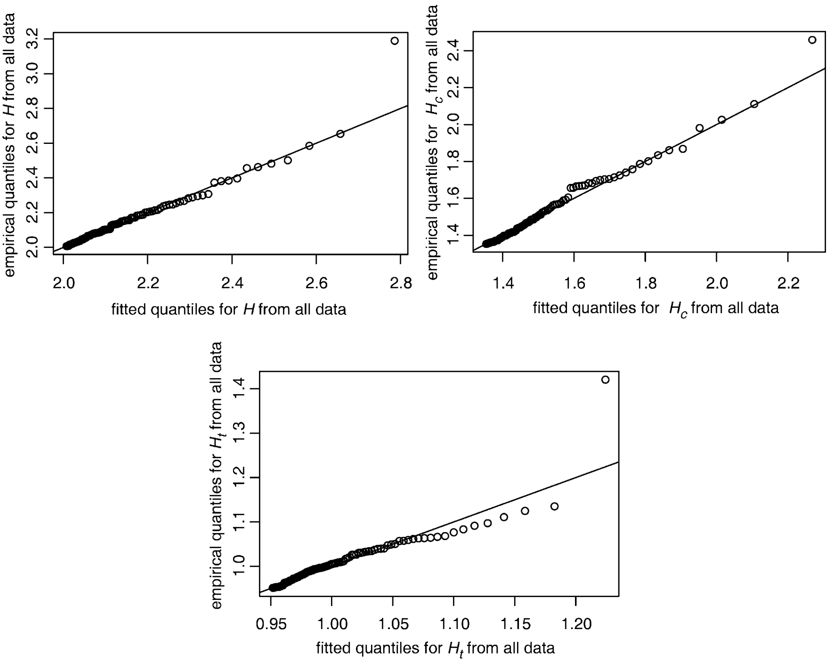

Fig. B2. Quantile–quantile plots of empirical distributions and GPD fits for combined dimensionless wave, crest and trough heights.

References

Al-Humoud, J., Tayfun, M.A., Askar, H., 2002. Distribution of nonlinear wave crests. Ocean Engineering 29, 1929–1943.

Coles, S., 2001. An Introduction to Statistical Modeling of Extreme Values, Series in Statistics. Springer, Berlin.

Embrechts, P., Klüppelberg, C., Mikosch, T., 1997. Modelling Extremal Events. Springer, Berlin.

Forristall, G.Z., 1978. On the statistical distribution of wave heights in a storm. Journal of Geophysical Research 830 (C5), 2353–2358.

Haring, R.E., Osborne, A.R., Spencer, L.P., 1976. Extreme wave parameters based on continental shelf storm wave records. In: Proceedings of the fifteenth Coastal Engineering Conference, Honolulu, USA, July 1976. American Society of Civil Engineers, pp. 151–170.

Krogstad, H.E., 1985. Height and period distribution of extreme waves. Applied Ocean Research 7 (3), 158–165.

Loader, C., 1999. Local Regression and Likelihood. Springer, Berlin, ISBN: 0-387-98775-4.

Massel, S.R., 1996. Ocean surface waves: their physics and prediction, Advanced series on ocean Engineering, vol. 11. World scientific Publishing, Singapore, ISBN: 9810216866.

Mori, N., Liu, P.C., Yasuda, T., 2002. Analysis of freak waves measurements in the sea of japan. Ocean Engineering 29, 1399–1414.

Nerzic,R., Prevosto, M., 1997. A Weibull-Stokes model for the distribution of maximum wave and crest heights. In: Proceedings of the Seventh (1997) International Offshore and Polar Engineering Conference, vol. 3, Honolulu, USA, May 1997. The International Society of Offshore and Polar Engineers. pp. 367–377.

Stansell, P., 2004. Distributions of freak wave heigths measured in the North Sea. Applied Ocean Research 26 (1–2), 35–48.

Stansell, P., Wolfram, J., Linfoot, B.T., 2002. Effect of sampling rate on wave height statistics. Ocean Engineering 29, 1023–1047.

Tayfun, M.A., 1981a. Breaking-limited wave heights. Journal of the Waterway, Port, Coastal and Ocean Division Proceedings of the American Society of Civil Engineers 107 (2), 59–69.

Tayfun, M.A., 1981b. Distribution of crest-to-trough wave heights. Journal of the Waterway, Port, Coastal and Ocean Division Proceedings of the American Society of Civil Engineers 107 (3), 149–158.

Tayfun, M.A., 1990. Distribution of large wave heights. Journal of the Waterway, Port, Coastal and Ocean Engineering 116 (6), 686–707.

Tung, C.C., Huang, N.E., 1985. Peak and trough distributions of nonlinear waves. Ocean Engineering 12, 201–209.

Yasuda, T., Mori, N., 1997. Occurrence properties of giant freak waves in sea area around japan. Journal of Waterway, Port, Coastal and Ocean Engineering 123 (4), 209–213.